*Journal of Geosciences,* 56 (2011), 257–271 DOI: 10.3190/jgeosci.100

Original paper

# Interesting supergene Pb-rich mineral association from the Rovnost mining field, Jáchymov (St. Joachimsthal), Czech Republic

Jiří SEJKORA[1*], Jakub PLÁŠIL[2], Ivana CÍSAŘOVÁ[3], Radek ŠKODA[4], Jan HLOUŠEK[5], František VESELOVSKÝ[6], Ivana JEBAVÁ[1]

[1] *Department of Mineralogy and Petrology, National Museum, Václavské nám. 68, 115 79 Prague 1, Czech Republic; jiri_sejkora@nm.cz*
[2] *Mineralogical Crystallography, Institute of Geological Sciences, University Bern, Freiestrasse 3, CH-3012 Bern, Switzerland*
[3] *Department of Inorganic Chemistry, Faculty of Science, Charles University, Hlavova 2030, 128 40 Prague 2, Czech Republic*
[4] *Institute of Geological Sciences, Masaryk University, Kotlářská 2, 611 37 Brno, Czech Republic*
[5] *U Roháčových kasáren 24, 100 00 Prague 10, Czech Republic*
[6] *Czech Geological Survey, Geologická 6, 152 00 Prague 5, Czech Republic*
[*] *Corresponding author*

Rich supergene mineral association with prevalence of Pb was found in a shallow gallery of the Rovnost mine, the Jáchymov (St. Joachimsthal) ore district, western Bohemia (Czech Republic). Mimetite occurs as colourless transparent flexible fibres up to 1 mm in length and up to 10 μm in diameter. The fibres form greyish white aggregates (up to 1 $cm^2$ in area) grown on the surface of gangue strongly affected by supergene alteration. The results of the single crystal X-ray diffraction study of mimetite with $R_1 = 0.0381$ are fully consistent with data reported previously for this mineral phase. According to electron microprobe study, interesting are namely elevated contents of $SiO_4$ (up to 0.16 *apfu*). Among the supergene minerals, cerussite, anglesite, wulfenite, philipsbornite–segnitite minerals, pyromorphite and metazeunerite were determined based on powder X-ray diffraction and electron microprobe analyses. The presence of U (~ 4 wt. % $UO_3$) and As (up to 4 wt. % $As_2O_5$) in wulfenite is particularly noteworthy. Characteristic of the studied mineral association are elevated and omnipresent contents of $F^-$. This mineral assemblage is considered to be a result of a long-term *in-situ* weathering in near-surface conditions.

*Keywords: supergene mineralization, mimetite, lead minerals, Jáchymov, Czech Republic*
*Received: 10 May 2011; accepted: 19 September 2011; handling editor: S. Mills*
*The online version of this article (doi: 10.3190/jgeosci.100) contains supplementary electronic material.*

## 1. Introduction

Lead arsenates are common minerals in oxidation zones of sulphide ore deposits and occurrences. The restricted stability of these minerals may play a significant role in the mobility of arsenic and lead in the near-surface environment. The investigation of crystal structures and chemical compositions of supergene As-bearing phases may lead to a better understanding of the geochemical behaviour of As and thereby help to elucidate mechanisms of transport and accumulation of arsenic in natural conditions (Williams 1990; Morin et al. 2001; Kolitsch and Pring 2001; Magalhães and Silva 2003; Krivovichev et al. 2006, and others).

An interesting supergene Pb-rich mineral association was discovered in the Rovnost mining field, Jáchymov ore district, western Bohemia, Czech Republic. The subsequent research work resulted in the discovery of a suite of many interesting minerals that had not been found in Jáchymov before. Preliminary results of this research have been presented at the IMA 2010 General Meeting in Budapest (Sejkora et al. 2010b).

## 2. Geological setting

The Jáchymov ore district, located in the vicinity of the namesake town, Jáchymov (St. Joachimsthal), is a classic example of an Ag + As + Co + Ni + Bi + U vein-type hydrothermal mineralization. The ore veins cut a complex of medium-grade metasedimentary rocks of Cambrian to Ordovician age, in the contact aureole of a Variscan granite pluton. The majority of ore minerals were deposited during Variscan mineralization from mesothermal fluids (Ondruš et al. 2003a, b). Primary and supergene mineralization in this district resulted in extraordinarily rich associations; more than 420 mineral species have been described to date (Ondruš et al. 1997, 2003c, e; Plášil et al. 2009b, 2010b, 2011; Sejkora et al. 2010a–c; Tvrdý and Plášil 2010).

The studied mineral association was found in the samples from the Rovnost mine mining area (50°22′18.421″N, 12°53′32.83″E), collected by two of the present authors (JH and FV) during late 1980's. Samples come from a shallow gallery which reached an alteration zone of the vein extraordinarily rich in Pb. They were found in a pillar remaining as an edge of the stope.

This is an interesting type of oxidation zone within near-surface or outcrop portions of the Jáchymov veins. To date, such an association has not been described and the current research resulted in additional data contributing to the complexity of the geochemical systems in the Jáchymov ore district. The previous finds and descriptions of supergene minerals and associations were focused mainly on very rich accumulations which originated from sub-recent alteration in the old mining adits and workings environment. As mentioned by Ondruš et al. (2003d), the majority of accessible outcrops of the veins show relatively simple mineral associations. The outcrop parts exhibit effects of a nearly complete leaching of ore components. Only sporadic occurrences of minerals bearing uranium (torbernite, autunite, uranophane, kasolite), bismuth minerals (bismutite, bismutoferrite), copper (malachite, mixite) and lead (anglesite, pyromorphite) were reported. Ondruš et al. (2003d) further noted that the typical weathering pattern of veins with increasing depth, starting with a leached oxidation, enriched oxidation and cementation zones above the primary occurrence formed by unaltered minerals, is known only at the Geschieber (Svornost mine), Geister and partly at the Červené veins (Rovnost mine). The find of parsonsite in the outcrop parts of the Červené veins, reported by Plášil et al. (2009c), is also connected with alteration of galena, which was found as grains in the gangue. Certainly, not all Pb can be of radiogenic origin, as was demonstrated by Škácha et al. (2009) and Plášil et al. (2010a) in the case of Pb–U minerals in the Příbram ore district. The currently studied mineral associations represent an *in-situ* supergene association, formed by replacement of primary phases, particularly of massive galena.

## 3. Experimental techniques

### 3.1. Morphological study

The surface morphology of the samples was studied with the optical microscope Nikon SMZ1500 in combination with the digital camera Nikon DXM1200F (National Museum, Prague), used for photography in incandescent light. For the observations of the morphology of the fine-crystalline phases, a Hitachi S3700N (National Museum, Prague) scanning electron microscope was used. The secondary electron images (SE) of the surface details were also taken using this equipment on gold-coated samples.

### 3.2. X-ray powder diffraction study

The X-ray powder diffraction patterns of studied mineral phases were obtained from hand-picked samples using a Bruker D8 Advance diffractometer with solid-state 1D LynxEye detector using Cu$K_\alpha$ radiation (National Museum, Prague). In order to minimize the background, the powdered samples were placed on the surface of a flat silicon wafer from acetone suspension.

Bruker program EVA was utilized for the phase analysis together with the ICDD database PDF2 (release 2009). X-ray powder diffraction data were processed using the Bruker program TOPAS 4.2., where the profile fitting was done using a Pseudovoigt profile shape function corrected for asymmetry (full-axial model). Obtained positions of the diffraction maxima were used for the refinement of the unit-cell parameters by the Celref program of the LMGP suite for Windows (Laugier and Bochu 2007), an algorithm based on least-squares method.

### 3.3. Single crystal X-ray diffraction study

A crystal of fibrous mimetite of dimensions $0.08 \times 0.07 \times 0.30$ mm was selected for X-ray diffraction experiment utilizing an Enraf Nonius single-crystal diffractometer with a CCD detector (Faculty of Science, Charles University, Prague). The unit-cell was refined from 9868 diffractions between 2.91 and 24.11 °θ by least-squares algorithm of the Collect software (Bruker AXS). The total number of diffractions measured was 13505. The three dimensional intensity data were corrected for background, Lorentz and polarization effects. Merging of equivalents gave 717 unique reflections. The $R_{int}$ of the data was 0.225. The crystal structure of fibrous mimetite has been solved from the data by direct methods using SIR92 (Altomare et al. 1994) and subsequently refined by full-matrix least-squares algorithm based on $F^2$ (SHELXL97, Sheldrick 2008); the final refinement was performed using JANA2006 (Petříček et al. 2006) and resulted in convergence with the following indices of agreement, $R_1 = 0.0381$, $wR_2 = 0.0866$ with a GOF = 2.50 for 292 observed reflections [$I_{obs} > 3\sigma(I)$]. Other details on data collection, crystal data and refinement are listed in the relevant table.

### 3.4. Chemical analyses

Quantitative chemical data for polished samples mounted in the epoxy resin were collected with a Cameca SX100 electron microprobe (Laboratory of Electron Microscopy and Microanalysis of the Masaryk University and Czech Geological Survey, Brno) operating in the wavelength-dispersion mode with an accelerating voltage of 15 kV, a specimen current of 8–10 nA, and a beam diameter of 5–10 μm. The following lines and standards were used: $K_\alpha$: andradite (Ca), albite (Na), almandine (Si), Cu (Cu), grossular (Al), fluorapatite (P), hematite (Fe), gahnite (Zn), NaCl (Cl), olivine (Mg), rhodonite (Mn), $SrSO_4$ (S), vanadinite (V), topaz (F); $L_\alpha$: lammerite (As), baryte (Ba),

**Fig. 1** White fine-crystalline aggregates of mimetite from Jáchymov on strongly altered supergene gangue. Width of area 7 mm, photo by J. Sejkora.

**Fig. 2** Aggregate of white fibrous mimetite crystals from Jáchymov. Width of area 3 mm, photo by J. Sejkora.

Sb (Sb), W (W); $M_\alpha$: galena (Pb), powellite (Mo) and $M_\beta$: Bi (Bi). Peak counting times were 20 s for main and 60 s for minor elements; each background was acquired for half of the peak time. Raw intensities were converted to the concentrations using automatic *PAP* matrix correction software package (Pouchou and Pichoir 1985). Elevated analytical totals of minerals containing a large amount of hydroxyl groups or crystal water are generally caused by water evaporation under high-vacuum conditions or water evaporation due to heating of the analyzed spot by the electron beam. Lower analytical totals for some samples are primarily caused by their porous nature or by poorly polished surfaces of soft or cryptocrystalline minerals.

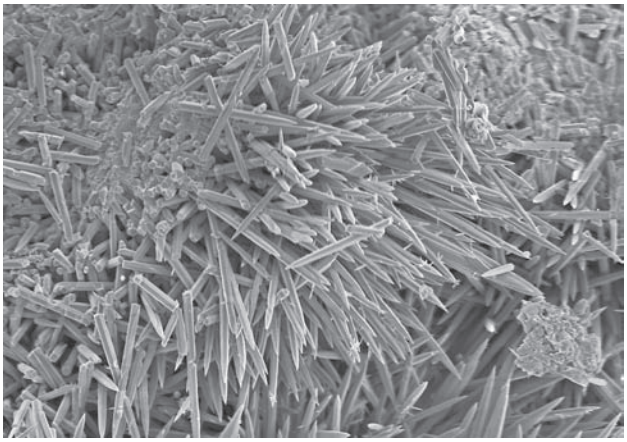

**Fig. 3** Aggregate of fibrous mimetite under the high magnification: long prismatic crystals of a micron thickness; SEM image, width of area is 70 μm.

## 4. Results and discussion

### *4.1. Mimetite*

Mimetite forms greyish white fine-crystalline aggregates (up to 1 $cm^2$ in the area) grown on the surface of strongly supergene-altered gangue (Figs 1–2). Individual mimetite crystals are represented by colourless transparent flexible fibres up to 1 mm in length and up to 10 μm in diameter (Fig. 3). In addition, mimetite forms locally abundant aggregates

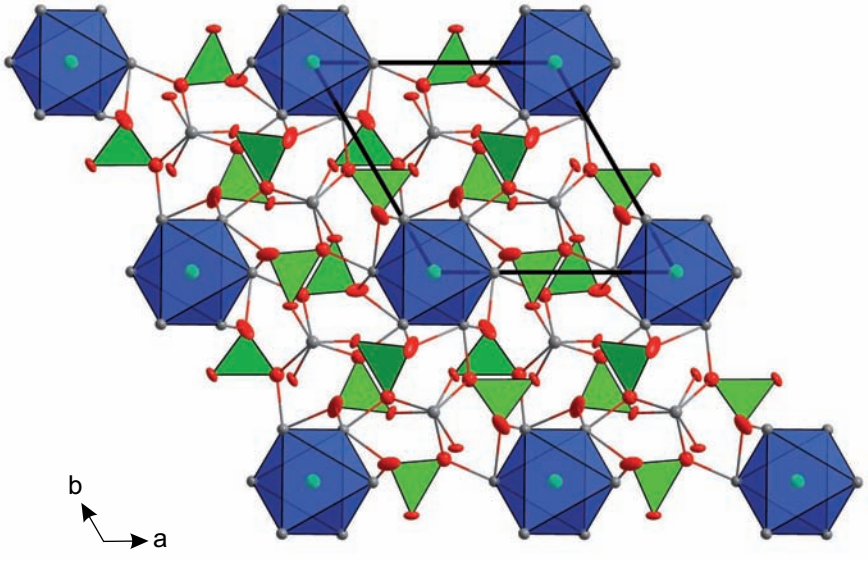


**Fig. 4** The crystal structure of fibrous mimetite from Jáchymov viewed along [001] direction. Green tetrahedra belong to $AsO_4^{3-}$ groups, $Pb^{2+}$ atoms are grey, O atoms red and Cl atoms green. The unit-cell edges are outlined. The atomic displacement ellipsoids represent 50% probability.

**Tab. 1** Refined unit-cell parameters of fibrous mimetite from Jáchymov in comparison with the published data (for hexagonal space group $P6_3/m$)

| Locality | Reference | $a$ [Å] | $c$ [Å] | $V$ [Å$^3$] |
|---|---|---|---|---|
| Jáchymov (CZ) | this paper, powder data | 10.24(2) | 7.4151(6) | 673(1) |
| Jáchymov (CZ) | this paper, single-crystal data | 10.2373(6) | 7.4257(4) | 673.97(7) |
| Durango, Mexico | Dai et al. (1991) | 10.212(2) | 7.419(4) | 669.90 |
| Geister vein, Jáchymov (CZ) | Ondruš et al. (1997) | 10.233(4) | 7.432(5) | 673.97 |
| Synthetic | Flis et al. (2010) | 10.2518(2) | 7.4482(2) | 677.93 |

**Tab. 2** Summary of data collection conditions and refinement parameters for fibrous mimetite

| Structural formula | $Pb_5(AsO_4)_3Cl$ |
|---|---|
| Unit-cell parameters (based on 9868 diffractions) | |
| $a$ = 10.2373(6)Å | |
| $c$ = 7.4257(4)Å | |
| $V$ = 673.97(7)Å$^3$ | |
| Z | 2 |
| Space group | $P6_3/m$ |
| Temperature | 293 K |
| Wavelength | Mo$K_a$, 0.7107 Å |
| Crystal dimensions (mm) | 0.08 × 0.07 × 0.30 |
| Collection mode | ω and Φ scans to fill an Ewald sphere |
| Limiting θ angles | 2.91-24.11° |
| Limiting Miller indices | $-11<h<11$, $-11<k<11$, $-8<l<8$ |
| No. of reflections | 13490 |
| No. of unique reflections | 392 |
| No. of observed reflections (criterion) | 292 [$I_{obs}>3\sigma(I)$] |
| Absorption correction (mm$^{-1}$), method | 70.08, analytical |
| $F_{000}$ | 1244 |
| Full-least square refinement by JANA2006 on $F^2$ | |
| Parameters refined | 35 |
| $R_1$ | 0.0381 |
| $wR_1$ | 0.0866 |
| $R_2$ | 0.0646 |
| $wR_2$ | 0.0916 |
| GOF# | 2.50 |
| $\Delta\sigma_{min}$, $\Delta\sigma_{max}$ (e/Å$^3$) | –3.09, 2.93 |
| Weighting scheme, details | σ, $w = 1/(\sigma^2(I) + 0.0004I^2)$ |

The *cif* file with a table of structure factors for mimetite from Jáchymov is deposited as electronic supplementary material of this paper at Journal web page *(http://dx.doi.org/10.3190/jgeosci.100)*.
# JANA2006 uses the weighting scheme based on the experimental expectations that do not force GOF to be one. Therefore, the values of GOF are usually larger than those from the SHELX program.

**Tab. 3** Atomic coordinates and displacement parameters [in Å$^2$] for the crystal structure of fibrous mimetite from Jáchymov

| Atom | x | y | z | $U_{eq}$ |
|---|---|---|---|---|
| Pb1 | 0.7491(2) | 0.7518(2) | 0.25 | 0.0307(6) |
| Pb2 | 0.666667 | 0.333333 | 0.0068(2) | 0.0292(5) |
| As3 | 0.3836(4) | 0.4079(4) | 0.25 | 0.0204(7) |
| Cl | 0.00 | 0.00 | 0.00 | 0.041(5) |
| O6 | 0.489(2) | 0.328(2) | 0.25 | 0.03(1) |
| O8 | 0.488(3) | 0.597(3) | 0.25 | 0.045(7) |
| O9 | 0.273(2) | 0.359(3) | 0.072(2) | 0.07(1) |

up to 200 μm across in altered gangue. These minerals replaced older aggregates of the segnitite–philipsbornite series minerals.

### 4.1.1. X-ray diffraction

Mimetite crystals were checked both using single crystal and powder XRD (Tab. 1). The unit-cell from the single-crystal data was refined from 9868 diffractions between 2.91 and 24.11 °θ by least-squares algorithm of the Collect software (Bruker AXS). The refined unit-cell parameters (Tab. 1) are consistent with those reported previously for mimetite samples (Dai et al. 1991). Unit-cell parameters refined from the powder data are similar to those obtained from single-crystal data and are comparable to those of mimetite with the As-rich part of the pyromorphite–mimetite solid solution series, in the current case > 80 mol. % As (see Flis et al. 2010). The refined crystal structure of currently studied mimetite (Tab. 2) is, within

**Tab. 4** Anisotropic displacement parameters for the crystal structure of fibrous mimetite from Jáchymov

| Atom | $U_{11}$ | $U_{22}$ | $U_{33}$ | $U_{12}$ | $U_{13}$ | $U_{23}$ |
|---|---|---|---|---|---|---|
| Pb1 | 0.0235(8) | 0.0244(8) | 0.0430(8) | 0.0110(7) | 0 | 0 |
| Pb2 | 0.0317(7) | 0.0317(7) | 0.0242(9) | 0.0158(3) | 0 | 0 |
| Cl | 0.045(6) | 0.045(6) | 0.033(9) | 0.023(3) | 0 | 0 |
| O6 | 0.04(2) | 0.04(1) | 0.03(1) | 0.03(1) | 0 | 0 |
| O9 | 0.08(1) | 0.10(2) | 0.06(1) | 0.07(1) | –0.05(1) | –0.05(1) |

The anisotropic displacement factor exponent takes the form: $-2\pi[ha\times U_{11} + ... + 2hka\times b\times U_{12}]$

**Tab. 5** Interatomic distances and selected geometrical parameters for the crystal structure of fibrous mimetite from Jáchymov

| | | | |
|---|---|---|---|
| Pb1–Cl (2×) | 3.1579(9) | Pb2–O1 (3×) | 2.55(2) |
| Pb1–O1 | 3.03(4) | Pb2–O2 (3×) | 2.79(3) |
| Pb1–O2 | 2.32(2) | Pb2–O3 (3×) | 2.95(4) |
| Pb1–O3 (2×) | 2.60(2) | <Pb2–O> | 2.76 |
| Pb1–O3 (2×) | 2.75(4) | | |
| <Pb1–O> | 2.68 | | |
| As–O1 | 1.64(3) | O1–O1 | 3.11(5) |
| As–O2 | 1.68(2) | O1–O2 | 2.75(4) |
| As–O3 (2×) | 1.65(2) | O1–O3 | 2.72(4) |
| <As–O> | 1.66 | O2–O3 | 2.68(3) |
| Δ | 0.00733 | O2–O3 | 3.11(4) |
| $\sigma^2$ | 5.8814 | O3–O3 | 2.65(3) |
| ECoN | 3.99 | | |

Δ, bond-length distortion after Brown and Shannon (1973); $\sigma^2$, bond-angle distortion (variance) after Robinson et al. (1971); ECoN, an effective coordination number after Hoppe (1979). Calculated utilizing Vesta software (Momma and Izumi 2008).

**Tab. 6** Bond-valence analysis for the crystal structure of mimetite from Jáchymov

| | Pb1 | Pb2 | As | ∑BV |
|---|---|---|---|---|
| O1 | 0.11 | 0.30×3↓ | 1.41 | 1.82 |
| O2 | 0.48 | 0.18×3↓ | 1.27 | 1.93 |
| O3 | 0.20×2↓, 0.27×2↓ | 0.13×3↓ | 1.37×2↓ | 1.98 |
| Cl | 0.18×2↓,×6→ | | | 1.10 |
| ∑BV | 1.91 | 1.86 | 5.42 | |

Values are expressed in valence units [*vu*]. Multiplicity is indicated by ×→, ×↓; $Pb^{2+}$–O bond strengths from Krivovichev and Brown (2001); $As^{5+}$–O bond strengths from Brown and Altermatt (1985); $Pb^{2+}$–$Cl^-$ bond strengths from Brese and O'Keeffe (1991).

the error, identical with the refinement of Dai et al. (1991). Atomic co-ordinates and displacement parameters, listed in Tabs 3–5, are consistent with previous crystal structure refinements. Crystal structure of the studied mimetite (Fig. 4) consists of $AsO_4$ tetrahedra, $PbO_9$ polyhedra, tri-capped trigonal prisms, and perfectly octahedrally coordinated $Cl^-$ in the cages formed by 6 Pb atoms (Pb1). Selected interatomic distances and other geometric parameters are listed in Tab. 6. According to the bond-valence analysis (Tab. 6) and the structure refinement, the formula of studied mimetite is $Pb_5(AsO_4)_3Cl$, Z = 2.

## 4.1.2. Chemical composition

Studied were chemical compositions of fibrous mimetite aggregates that were examined by XRD methods and mimetite aggregates that strongly push back older segnitite–philipsbornite (Tab. 7). Fibrous aggregates are especially interesting by their ($SiO_4$) contents of 0.08–0.16 *pfu* and ($PO_4$) contents of 0.11–0.32 *pfu* (Fig. 5). The empirical formula on the basis of As + P + Si + S = 3 is:

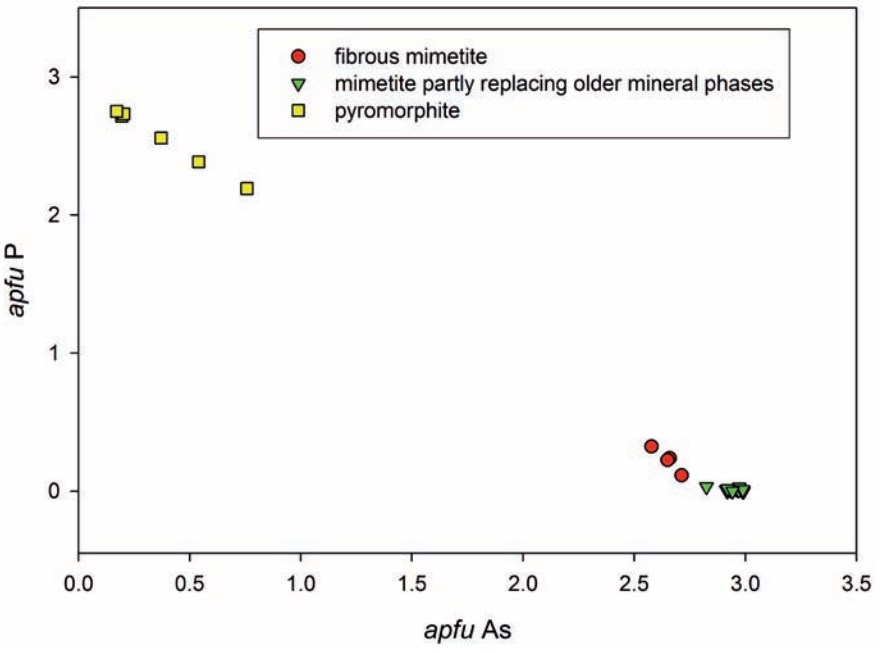


**Fig. 5** Plot of As vs. P contents (*apfu*) for minerals of the mimetite–pyromorphite series, Jáchymov.

**Tab. 7** Chemical composition of mimetite from Jáchymov (wt. % and *apfu*)

| | mean 1–3 | 1 | 2 | 3 | 4 | 5 | 6 | 7 | 8 |
|---|---|---|---|---|---|---|---|---|---|
| PbO | 75.92 | 77.10 | 76.44 | 74.20 | 76.39 | 76.28 | 74.97 | 73.37 | 75.68 |
| CuO | 0.00 | 0.00 | 0.00 | 0.00 | 0.15 | 0.00 | 0.10 | 0.21 | 0.09 |
| ZnO | 0.00 | 0.00 | 0.00 | 0.00 | 0.00 | 0.08 | 0.32 | 0.94 | 0.00 |
| $SiO_2$ | 0.45 | 0.33 | 0.65 | 0.35 | 0.00 | 0.05 | 0.00 | 0.09 | 0.00 |
| $As_2O_5$ | 20.13 | 19.46 | 20.90 | 20.03 | 22.36 | 22.18 | 22.13 | 22.59 | 22.03 |
| $P_2O_5$ | 1.05 | 1.50 | 0.54 | 1.11 | 0.00 | 0.07 | 0.13 | 0.04 | 0.07 |
| $SO_3$ | 0.07 | 0.08 | 0.07 | 0.06 | 0.04 | 0.08 | 0.00 | 0.00 | 0.34 |
| Cl | 2.19 | 2.20 | 2.17 | 2.20 | 2.15 | 2.11 | 2.18 | 1.79 | 2.08 |
| F | 0.10 | 0.09 | 0.10 | 0.11 | 0.38 | 0.43 | 0.48 | 0.50 | 0.43 |
| $H_2O$* | 0.11 | 0.25 | 0.05 | 0.02 | 0.31 | 0.22 | 0.13 | 0.13 | 0.14 |
| F + Cl = O | –0.54 | –0.54 | –0.53 | –0.54 | –0.64 | –0.66 | –0.69 | –0.61 | –0.65 |
| Total | 99.48 | 100.49 | 100.37 | 97.55 | 101.14 | 100.85 | 99.75 | 99.04 | 100.21 |
| $Pb^{2+}$ | 5.146 | 5.258 | 5.109 | 5.072 | 5.263 | 5.235 | 5.185 | 4.967 | 5.166 |
| $Cu^{2+}$ | 0.000 | 0.000 | 0.000 | 0.000 | 0.030 | 0.000 | 0.020 | 0.040 | 0.017 |
| $Zn^{2+}$ | 0.000 | 0.000 | 0.000 | 0.000 | 0.000 | 0.015 | 0.061 | 0.174 | 0.000 |
| Σ Me-sites | 5.146 | 5.258 | 5.109 | 5.072 | 5.292 | 5.250 | 5.266 | 5.181 | 5.183 |
| $Si^{4+}$ | 0.112 | 0.085 | 0.161 | 0.090 | 0.000 | 0.013 | 0.000 | 0.022 | 0.000 |
| $As^{5+}$ | 2.650 | 2.578 | 2.713 | 2.659 | 2.992 | 2.956 | 2.972 | 2.970 | 2.920 |
| $P^{5+}$ | 0.224 | 0.322 | 0.114 | 0.239 | 0.000 | 0.016 | 0.028 | 0.007 | 0.015 |
| $S^{6+}$ | 0.013 | 0.016 | 0.012 | 0.012 | 0.008 | 0.015 | 0.000 | 0.000 | 0.065 |
| Σ T-sites | 3.000 | 3.000 | 3.000 | 3.000 | 3.000 | 3.000 | 3.000 | 3.000 | 3.000 |
| Cl | 0.934 | 0.943 | 0.912 | 0.948 | 0.931 | 0.911 | 0.948 | 0.765 | 0.894 |
| F | 0.080 | 0.075 | 0.076 | 0.089 | 0.303 | 0.344 | 0.392 | 0.394 | 0.345 |
| OH | 0.185 | 0.422 | 0.083 | 0.034 | 0.529 | 0.374 | 0.223 | 0.218 | 0.237 |
| Σ X-sites | 1.199 | 1.441 | 1.071 | 1.071 | 1.764 | 1.629 | 1.563 | 1.376 | 1.475 |

1–3: mean and point analyses of mimetite fibrous aggregates; 4–8 representative analyses of mimetite aggregates replacing older segnitite or philipsbornite. Coefficients of empirical formulae were calculated assuming (As + P + S + Si) = 3; $H_2O$* contents were calculated on the basis of charge balance.

$Pb_{5.15}[(AsO_4)_{2.65}(PO_4)_{0.23}(SiO_4)_{0.11}(SO_3)_{0.01}]_{\Sigma 3.00}[Cl_{0.93}F_{0.08}(OH)_{0.18}]_{\Sigma 1.19}$.

Mimetite aggregates partly replacing older phases contain irregularly elevated abundances of Cu and Zn (up to 0.22 *apfu*). The tetrahedral sites contain low P and Si (up to 0.03 *apfu*) and high S (up to 0.14 *apfu*). Remarkable in these aggregates are elevated contents of F (up to 0.42 *apfu*), which are uncommon in minerals of the mimetite–pyromorphite series. Representative analyses of this mimetite type and coefficients of the empirical formulae are presented in Tab. 7.

## 4.2. Cerussite

Cerussite forms tiny colourless twinned crystals up to 0.5 mm in size in cavities of altered quartz gangue as well as aggregates in association with anglesite and sphalerite. Its refined unit-cell parameters (Tab. 8) from the X-ray powder diffraction data are consistent with those published for cerussite from other occurrences.

## 4.3. Anglesite

Anglesite was found in the samples of strongly altered primary minerals. It forms a part of the irregular whitish grey thick crusts (up to 2 mm thick) covering massive galena in association with cerussite and sphalerite.

X-ray powder diffraction data for anglesite from the association studied matches very well the reference patterns from the ICDD PDF2 database. The refined unit-cell parameters are consistent with data published for this mineral species (Tab. 9).

**Tab. 8** Refined unit-cell parameters for cerussite from Jáchymov in comparison with the published data (for orthorhombic space group *Pmcn*)

| | this paper | Příbram, Chevrier et al. (1992)[1] | synt., Antao and Hassan (2009)[2] |
|---|---|---|---|
| *a* [Å] | 5.173(2) | 5.179(1) | 5.18324(2) |
| *b* [Å] | 8.487(2) | 8.492(3) | 8.49920(3) |
| *c* [Å] | 6.135(2) | 6.141(2) | 6.14746(3) |
| *V* [Å$^3$] | 269.3(2) | 270.08 | 270.817(2) |

[1]neutron single-crystal diffraction data
[2]high-resolution synchrotron powder diffraction

**Tab. 9** Refined unit-cell parameters for anglesite from Jáchymov in comparison with the published data (for orthorhombic space group *Pbnm*)

| | this paper | Jacobsen et al. (1998) | Miyake et al. (1978) |
|---|---|---|---|
| *a* [Å] | 6.953(2) | 6.9549(9) | 6.959(2) |
| *b* [Å] | 8.476(2) | 8.472(1) | 8.482(2) |
| *c* [Å] | 5.386(2) | 5.3973(8) | 5.398(2) |
| *V* [Å$^3$] | 317.4(1) | 318.03(8) | 318.6 |

## 4.4. Wulfenite

Wulfenite was found as pale brown crystals up to 0.2 mm in size in cavities of strongly corroded quartz gangue in association with metazeunerite, green pyromorphite and fibrous mimetite.

The study of the chemical composition of wulfenite (Tab. 10) proved the presence of some additional minor elements besides dominant Pb and Mo. The Pb cation site contains low amounts of Fe (up to 0.005 *apfu*) and U (0.03–0.05 *apfu*). The presence of up to ~4 wt. % $UO_3$ (probably in the form of the uranyl ion $(UO_2)^{2+}$) in the cation site is indicated by correlation of U vs. Pb + Fe (Fig. 6). The anion site contains minor W (up to 0.001 *apfu*) and up to ~4 wt. % $As_2O_5$ (0.10–0.13 *apfu*) in addition to the dominant Mo. The empirical formula of wulfenite from Jáchymov based on Pb + U + Mo + As = 2 *apfu* is $[Pb_{0.96}(UO_2)_{0.04}]_{\Sigma 1.00}[(MoO_4)_{0.87}(AsO_4)_{0.12}]_{\Sigma 0.99}$. To our knowledge, such elevated contents of U and As in wulfenite were not reported in the literature. Its refined unit-cell parameters (Tab. 11) are smaller than the literature data. This possibly reflects a $(MoO_4)^{2-} \leftrightarrow (AsO_4)^{3-}$ substitution, with $AsO_4$ tetrahedra having a smaller volume. However, the direct mechanism is not clear as yet; the above-mentioned substitution should be accompanied by compensation of positive charge.

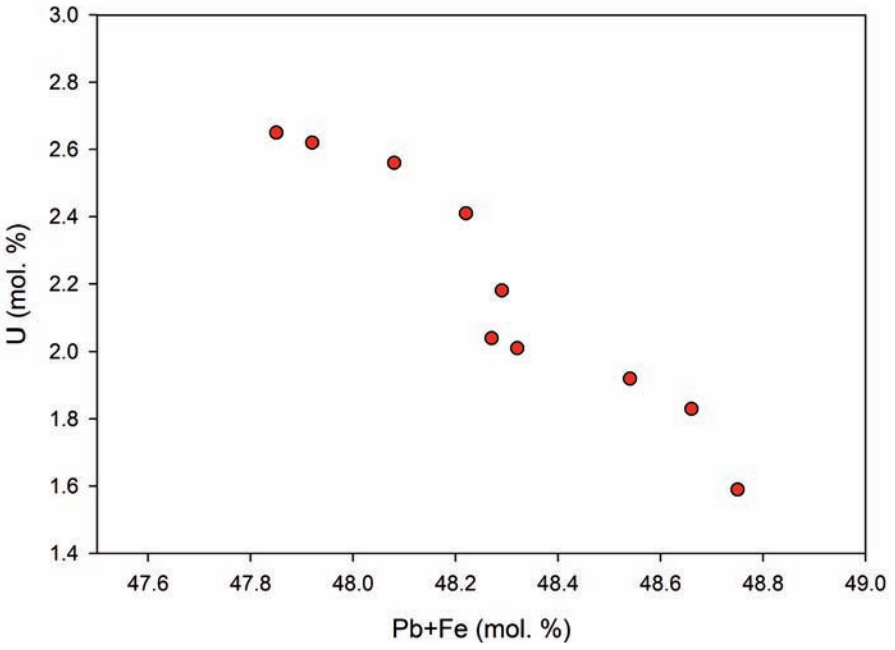


**Fig. 6** Plot of Pb + Fe vs. U contents (mol. %) in wulfenite from Jáchymov.

**Tab. 10** Chemical composition of wulfenite from Jáchymov (wt. % and *apfu*)

| | mean | 1 | 2 | 3 | 4 | 5 | 6 | 7 | 8 | 9 |
|---|---|---|---|---|---|---|---|---|---|---|
| FeO | 0.06 | 0.06 | 0.10 | 0.09 | 0.08 | 0.08 | 0.07 | 0.03 | 0.04 | 0.03 |
| PbO | 57.98 | 58.34 | 58.06 | 58.12 | 57.50 | 57.92 | 57.79 | 57.62 | 57.54 | 58.90 |
| $As_2O_5$ | 3.66 | 3.25 | 3.39 | 3.37 | 3.83 | 3.66 | 3.92 | 4.06 | 3.62 | 3.85 |
| $UO_3$ | 3.37 | 3.12 | 2.96 | 2.45 | 3.12 | 2.81 | 3.95 | 4.05 | 4.09 | 3.78 |
| $MoO_3$ | 33.87 | 34.71 | 34.13 | 34.12 | 33.50 | 33.56 | 33.50 | 33.28 | 33.92 | 34.13 |
| $WO_3$ | 0.04 | 0.02 | 0.08 | 0.03 | 0.07 | 0.04 | 0.00 | 0.09 | 0.04 | 0.01 |
| Total | 98.99 | 99.50 | 98.72 | 98.18 | 98.10 | 98.07 | 99.23 | 99.13 | 99.25 | 100.70 |
| $Fe^{2+}$ | 0.003 | 0.003 | 0.005 | 0.005 | 0.004 | 0.004 | 0.004 | 0.002 | 0.002 | 0.002 |
| $Pb^{2+}$ | 0.962 | 0.963 | 0.966 | 0.970 | 0.961 | 0.969 | 0.958 | 0.957 | 0.955 | 0.963 |
| $U^{6+}$ | 0.044 | 0.040 | 0.038 | 0.032 | 0.041 | 0.037 | 0.051 | 0.052 | 0.053 | 0.048 |
| Pb + Fe + U | 1.009 | 1.007 | 1.009 | 1.007 | 1.006 | 1.010 | 1.013 | 1.011 | 1.010 | 1.013 |
| $As^{5+}$ | 0.118 | 0.104 | 0.109 | 0.109 | 0.124 | 0.119 | 0.126 | 0.131 | 0.117 | 0.122 |
| $Mo^{6+}$ | 0.872 | 0.889 | 0.880 | 0.883 | 0.868 | 0.871 | 0.861 | 0.857 | 0.873 | 0.865 |
| $W^{6+}$ | 0.001 | 0.000 | 0.001 | 0.000 | 0.001 | 0.001 | 0.000 | 0.001 | 0.001 | 0.000 |
| Mo + W + As | 0.991 | 0.993 | 0.991 | 0.993 | 0.994 | 0.990 | 0.987 | 0.989 | 0.990 | 0.987 |

Coefficients of empirical formulae were calculated on the basis of 2 *apfu*.

**Tab. 11** Refined unit-cell parameters of wulfenite from Jáchymov (for tetragonal space group $I4_1/a$)

| | this paper | Secco et al. (2008) | Lugli et al. (1999) |
|---|---|---|---|
| *a* [Å] | 5.421(4) | 5.433(1) | 5.434 |
| *c* [Å] | 12.12(2) | 12.098(1) | 12.107 |
| *V* [Å$^3$] | 356.2(8) | 357.1(1) | 357.5 |

## 4.5. Philipsbornite–segnitite series

Minerals of the philipsbornite–segnitite series form irregular microcrystalline crusts (Fig. 7) up to 1 cm in size, in cavities of strongly altered quartz gangue, with greyish white, yellow green to olive green colour (Fig. 8). They

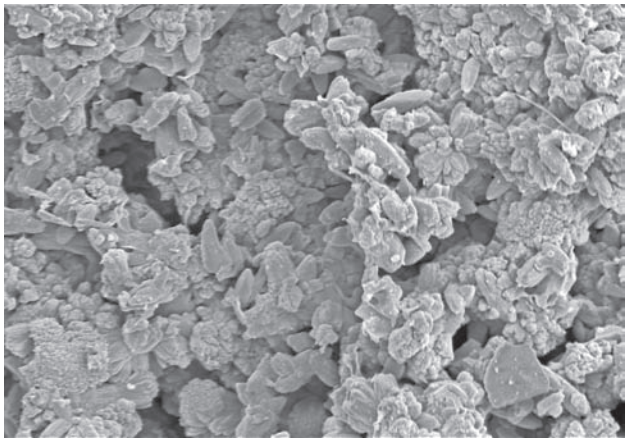

**Fig. 7** Crystalline crusts of the minerals of segnitite–philipsbornite series; SEM image, width of area is 60 μm.

**Fig. 8** Olive-green microcrystalline aggregates of the segnitite–philipsbornite series minerals in cavity of strongly supergene altered quartz gangue, Jáchymov. Width of area 10 mm, photo by J. Sejkora.

are often intensively replaced by younger aggregates of mimetite and pyromorphite.

The minerals were identified by X-ray powder diffraction data; lower values of refined unit-cell parameters for philipsbornite from Jáchymov (Tab. 12) are probably caused by minor contents of P and Si (e.g., Sejkora et al. 2001a). The refined unit-cell parameters for segnitite from Jáchymov (Tab. 12) are similar to those of the segnitite–beudantite series (Fig. 9).

Chemical compositions of minerals of philipsbornite–segnitite series are given in Tab. 13. The low Fe (up to 1.09 *apfu*) and high Al (2.15–2.82 *apfu*) contents are

**Tab. 12** Refined unit-cell parameters for the minerals of philipsbornite–segnitite series from Jáchymov in comparison with the literature data

| Mineral | Locality | Reference | *a* (Å) | *c* (Å) | *c*/*a* | *V* (Å$^3$) |
|---|---|---|---|---|---|---|
| philipsbornite | Jáchymov | this paper | 7.068(7) | 17.0376(3) | 2.411 | 732.2(7) |
| philipsbornite | Moldava | Sejkora et al. (1998) | 7.073(7) | 17.13(4) | 2.423 | 742.6 |
| philipsbornite | Cínovec | David et al. (1990) | 7.14 | 17.13 | 2.399 | 756.3 |
| philipsbornite | Tsumeb | Schmetzer et al. (1982) | 7.174 | 17.18 | 2.395 | 765.7 |
| philipsbornite | Dundas | Walenta et al. (1982) | 7.11 | 17.05 | 2.398 | 796.4 |
| segnitite | Jáchymov | this paper | 7.320(4) | 17.1332(2) | 2.341 | 795.0(5) |
| segnitite | Moldava | Sejkora et al. (2001a) | 7.373(1) | 17.108(4) | 2.320 | 805.4(2) |
| segnitite | Cínovec | Jansa et al. (1998) | 7.348(3) | 17.09(1) | 2.325 | 799.1 |
| segnitite | Štěpánov | Sejkora et al. (2001b) | 7.382(1) | 17.119(3) | 2.336 | 807.8(2) |
| segnitite | Broken Hill | Mills (2007) | 7.303 | 17.108 | 2.343 | 804.8 |
| segnitite | Schwarzwald | Walenta (1966) | 7.36 | 17.21 | 2.338 | 807 |
| segnitite | Broken Hill | Birch et al. (1992) | 7.359(3) | 17.113(8) | 2.325 | 802.6(6) |
| segnitite | Broken Hill | Rattray et al. (1996) | 7.335(5) | 17.11(2) | 2.333 | 797(1) |
| segnitite | St. Andreasberg | Bischoff (1999) | 7.376(1) | 17.145(2) | 2.324 | 807.8 |
| segnitite | Pützbach | Bischoff (1999) | 7.364(1) | 17.145(4) | 2.328 | 805.2 |
| beudantite (Cu) | Krupka | Sejkora et al. (2009) | 7.3265(7) | 17.097(2) | 2.334 | 794.8(1) |
| beudantite | Tsumeb | Szymański (1988) | 7.3151(9) | 17.0355(5) | 2.329 | 789.5 |
| beudantite | Tsumeb | Szymański (1988) | 7.3125(8) | 17.0217(7) | 2.328 | 788.3 |
| beudantite | Dernbach | Giuseppetti and Tadini (1989) | 7.339(1) | 17.034(1) | 2.321 | 794.6 |
| beudantite | Broken Hill | Rattray et al. (1996) | 7.345(7) | 17.06(2) | 2.323 | 796(2) |
| beudantite | Broken Hill | Rattray et al. (1996) | 7.315(5) | 17.07(2) | 2.334 | 791(2) |
| beudantite | Cínovec | Sejkora et al. (2001a) | 7.3713(9) | 17.076(2) | 2.317 | 803.5(1) |
| beudantite | Moldava | Sejkora et al. (2001a) | 7.346(1) | 17.012(5) | 2.316 | 795.0(3) |
| beudantite | Moldava | Sejkora et al. (2001a) | 7.351(2) | 17.028(8) | 2.316 | 796.8(5) |

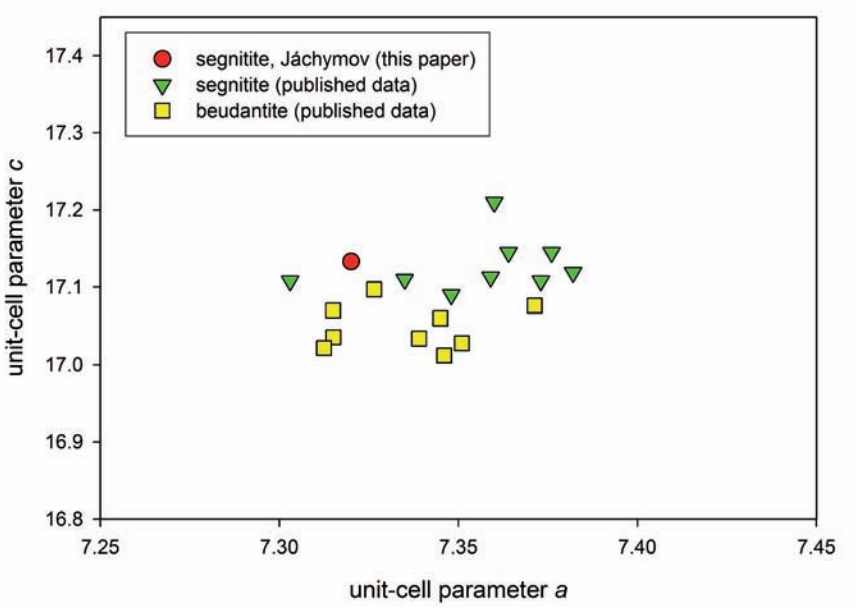


**Fig. 9** Plot of unit-cell parameters *a* and *c* for minerals of the segnitite–beudantite series. For references to the published data see Tab. 13.

**Tab. 13** Chemical composition of minerals of the philipsbornite–segnitite series from Jáchymov (wt. % and *apfu*)

| | segnitite | | | | philipsbornite | | | | | |
|---|---|---|---|---|---|---|---|---|---|---|
| | 1 | 2 | 3 | 4 | 5 | 6 | 7 | 8 | 9 | 10 |
| CaO | 0.00 | 0.02 | 0.00 | 0.00 | 0.08 | 0.00 | 0.00 | 0.22 | 0.07 | 0.04 |
| PbO | 31.26 | 30.69 | 29.67 | 28.04 | 33.05 | 33.91 | 34.58 | 37.69 | 36.90 | 35.15 |
| CuO | 1.88 | 1.43 | 0.30 | 0.00 | 0.47 | 0.25 | 0.53 | 0.06 | 0.15 | 0.28 |
| ZnO | 0.22 | 0.31 | 0.52 | 0.19 | 0.39 | 0.28 | 0.31 | 0.26 | 0.28 | 0.43 |
| $Al_2O_3$ | 2.12 | 2.27 | 2.13 | 0.26 | 18.81 | 17.99 | 19.33 | 19.28 | 18.57 | 16.51 |
| $Fe_2O_3$ | 26.75 | 26.56 | 29.21 | 28.43 | 2.83 | 3.48 | 2.16 | 3.58 | 5.82 | 7.45 |
| $SiO_2$ | 1.19 | 1.31 | 2.22 | 0.11 | 0.15 | 0.10 | 0.22 | 0.50 | 0.09 | 1.04 |
| $As_2O_5$ | 24.43 | 25.41 | 19.44 | 27.51 | 27.34 | 26.78 | 27.18 | 24.81 | 22.57 | 29.47 |
| $P_2O_5$ | 0.36 | 0.18 | 0.41 | 0.08 | 1.65 | 1.50 | 1.82 | 3.56 | 6.74 | 1.78 |
| $SO_3$ | 0.69 | 0.38 | 4.61 | 0.00 | 0.40 | 0.42 | 0.22 | 1.89 | 0.47 | 0.24 |
| F | 0.28 | 0.31 | 0.13 | 0.00 | 0.79 | 0.73 | 0.76 | 0.75 | 0.38 | 0.14 |
| $H_2O$* | 9.02 | 8.80 | 8.46 | 7.80 | 8.85 | 8.87 | 9.14 | 9.18 | 9.62 | 9.03 |
| O = F | –0.12 | –0.13 | –0.06 | 0.00 | –0.33 | –0.31 | –0.32 | –0.32 | –0.16 | –0.06 |
| Total | 98.08 | 97.53 | 97.04 | 92.42 | 94.48 | 94.00 | 95.93 | 101.47 | 101.49 | 101.50 |
| $Ca^{2+}$ | 0.000 | 0.003 | 0.000 | 0.000 | 0.011 | 0.000 | 0.000 | 0.026 | 0.009 | 0.004 |
| $Pb^{2+}$ | 1.139 | 1.099 | 0.987 | 1.037 | 1.102 | 1.164 | 1.154 | 1.133 | 1.107 | 1.044 |
| Σ A-site | 1.139 | 1.102 | 0.987 | 1.037 | 1.113 | 1.164 | 1.154 | 1.160 | 1.116 | 1.048 |
| $Cu^{2+}$ | 0.192 | 0.143 | 0.028 | 0.000 | 0.044 | 0.024 | 0.050 | 0.005 | 0.013 | 0.023 |
| $Zn^{2+}$ | 0.022 | 0.031 | 0.047 | 0.019 | 0.036 | 0.026 | 0.028 | 0.021 | 0.023 | 0.035 |
| $Al^{3+}$ | 0.338 | 0.356 | 0.310 | 0.042 | 2.747 | 2.703 | 2.824 | 2.537 | 2.440 | 2.146 |
| $Fe^{3+}$ | 2.723 | 2.659 | 2.716 | 2.939 | 0.264 | 0.334 | 0.201 | 0.301 | 0.488 | 0.619 |
| Σ B-site | 3.275 | 3.189 | 3.100 | 3.000 | 3.091 | 3.087 | 3.103 | 2.865 | 2.963 | 2.823 |
| $Si^{4+}$ | 0.161 | 0.174 | 0.274 | 0.016 | 0.019 | 0.013 | 0.027 | 0.056 | 0.010 | 0.114 |
| $As^{5+}$ | 1.728 | 1.768 | 1.256 | 1.975 | 1.771 | 1.785 | 1.761 | 1.449 | 1.315 | 1.699 |
| $P^{5+}$ | 0.041 | 0.020 | 0.043 | 0.009 | 0.173 | 0.162 | 0.191 | 0.337 | 0.636 | 0.166 |
| $S^{6+}$ | 0.070 | 0.038 | 0.427 | 0.000 | 0.037 | 0.040 | 0.020 | 0.158 | 0.039 | 0.020 |
| Σ T-site | 2.000 | 2.000 | 2.000 | 2.000 | 2.000 | 2.000 | 2.000 | 2.000 | 2.000 | 2.000 |
| $H^+$ | 8.140 | 7.810 | 6.972 | 7.146 | 7.314 | 7.544 | 7.556 | 6.839 | 7.152 | 6.643 |
| H* | 1.230 | 1.239 | 0.834 | 1.052 | 1.094 | 1.136 | 1.161 | 1.058 | 1.086 | 1.142 |
| OH | 6.906 | 6.572 | 6.136 | 6.091 | 6.222 | 6.409 | 6.394 | 5.782 | 6.069 | 5.504 |
| F | 0.121 | 0.128 | 0.052 | 0.000 | 0.310 | 0.294 | 0.298 | 0.265 | 0.133 | 0.050 |
| Σ X-site | 7.027 | 6.701 | 6.187 | 6.091 | 6.532 | 6.704 | 6.692 | 6.047 | 6.202 | 5.554 |

Representative analyses of segnitite (1–4) and philipsbornite (5–10) from Jáchymov;
$H_2O$* content calculated on the basis of ideal formula and charge balance;
H* content of $H^+$ bound in the group $(AsO_3OH)^{2-}$ calculated on the basis of charge balance;
coefficients of empirical formulae were calculated assuming (As + P + S + Si) = 2 *apfu*.

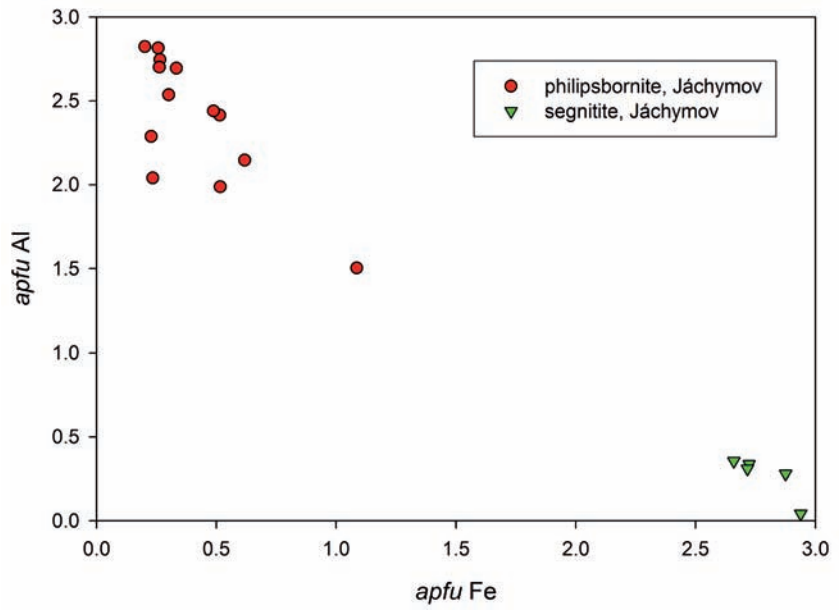


**Fig. 10** Plot of Fe and Al contents (*apfu*) in minerals of philipsbornite–segnitite series from Jáchymov.

typical of philipsbornite (Fig. 10). On the other hand, segnitite is characterized by only 0.04–0.36 *apfu* Al. In this site were also determined minor Cu (up to 0.21 *apfu*) and Zn (up to 0.08 *apfu*). In tetrahedral anion-sites (Fig. 11), segnitite is virtually P-free (up to 0.04 *apfu*), with Si (up to 0.27) and S (up to 0.42 *apfu*) contents; philipsbornite contains P (up to 0.64), Si (up to 0.34) and S (up to 0.16 *apfu*). Interesting are elevated F contents in segnitite (up to 0.13 *apfu*) and especially in philipsbornite (up to 0.37 *apfu*). Similar fluorine concentrations in minerals of the segnitite–beudantite series from the Krupka deposit were reported by Sejkora et al. (2009).

## 4.6. Pyromorphite

Pyromorphite was found as light green crystalline aggregates and irregular prismatic crystals up to 0.5 mm across in association with younger white mimetite and other supergene minerals. The pyromorphite was identified by powder X-ray diffraction. The refined unit-cell parameters (Tab. 14) are similar to those reported for the P-dominant members of the pyromorphite–mimetite series, namely those containing *c.* 10–20 mol. % As (Flis et al. 2010).

The chemical analyses (Tab. 15) yield 0.17–0.76 *apfu* As (Fig. 5), in addition to dominant P, and minor S and Si (up to 0.06 and 0.04 *apfu,* respectively). Interesting is the elevated F (0.25–0.32 *apfu*), unusual in minerals of the mimetite–pyromorphite series. The average empirical formula of pyromorphite on the basis of P + As + S + Si = 3 *apfu* is $Pb_{5.54}[(PO_4)_{2.56}(AsO_4)_{0.37}(SO_4)_{0.05}(SiO_4)_{0.02}]_{\Sigma 3.00}[Cl_{1.02}F_{0.29}(OH)_{0.80}]_{\Sigma 2.11}$.

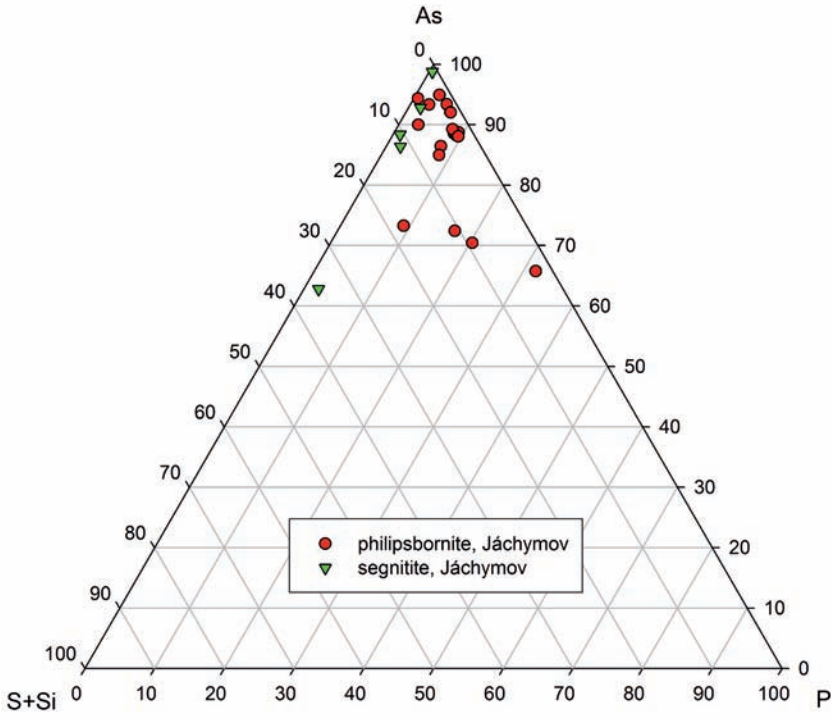


**Fig. 11** Ternary plot of anion-site occupancy (mol. units) in minerals of philipsbornite–segnitite series from Jáchymov.

**Tab. 14** Refined unit-cell parameters for pyromorphite from Jáchymov compared to published data (for hexagonal space group $P6_3/m$)

| Mineral | Reference | *a* [Å] | *c* [Å] | *V* [Å$^3$] |
|---|---|---|---|---|
| pyromorphite | Jáchymov, this paper | 10.061(1) | 7.381(1) | 647.0(1) |
| pyromorphite | Dai and Hughes (1989) | 9.997(1) | 7.351(2) | 633.62 |
| pyromorphite | Ondruš et al. (1997) | 9.926(3) | 7.292(5) | 622.19 |
| pyromorphite | Ondruš et al. (1997) | 9.875(3) | 7.218(6) | 609.57 |
| pyromorphite | Hashimoto and Matsumoto (1998) | 10.022(3) | 7.348(9) | 639.16 |
| pyromorphite | Hashimoto and Matsumoto (1998) | 9.993(2) | 7.334(6) | 634.25 |
| pyromorphite | Plášil et al. (2009a) | 10.051(3) | 7.373(2) | 645.1(3) |
| pyromorphite | Flis et al. (2010) | 9.9938(1) | 7.3397(1) | 634.85 |

**Tab. 15** Chemical composition of pyromorphite from Jáchymov (wt. %)

| | mean | 1 | 2 | 3 | 4 | 5 |
|---|---|---|---|---|---|---|
| CaO | 0.01 | 0.02 | 0.03 | 0.00 | 0.01 | 0.01 |
| PbO | 80.95 | 82.74 | 82.27 | 80.49 | 80.07 | 79.16 |
| $SiO_2$ | 0.08 | 0.15 | 0.05 | 0.07 | 0.06 | 0.09 |
| $As_2O_5$ | 2.79 | 1.48 | 1.54 | 1.31 | 5.55 | 4.09 |
| $P_2O_5$ | 11.89 | 12.70 | 12.74 | 12.94 | 9.92 | 11.15 |
| $SO_3$ | 0.27 | 0.28 | 0.27 | 0.32 | 0.18 | 0.28 |
| Cl | 2.37 | 2.29 | 2.42 | 2.39 | 2.44 | 2.31 |
| F | 0.36 | 0.39 | 0.35 | 0.31 | 0.36 | 0.40 |
| $H_2O$* | 0.47 | 0.58 | 0.56 | 0.39 | 0.51 | 0.29 |
| O = F + Cl | –0.69 | –0.68 | –0.69 | –0.67 | –0.70 | –0.69 |
| Total | 98.50 | 99.94 | 99.53 | 97.54 | 98.39 | 97.09 |
| $Ca^{2+}$ | 0.004 | 0.004 | 0.008 | 0.000 | 0.003 | 0.002 |
| $Pb^{2+}$ | 5.536 | 5.624 | 5.610 | 5.440 | 5.624 | 5.384 |
| Σ Me-sites | 5.539 | 5.629 | 5.619 | 5.440 | 5.626 | 5.386 |
| $Si^{4+}$ | 0.021 | 0.037 | 0.013 | 0.018 | 0.016 | 0.021 |
| $As^{5+}$ | 0.371 | 0.195 | 0.203 | 0.172 | 0.758 | 0.541 |
| $P^{5+}$ | 2.557 | 2.715 | 2.731 | 2š.750 | 2.192 | 2.385 |
| $S^{6+}$ | 0.051 | 0.053 | 0.052 | 0.060 | 0.034 | 0.053 |
| Σ T-sites | 3.000 | 3.000 | 3.000 | 3.000 | 3.000 | 3.000 |
| Cl | 1.019 | 0.980 | 1.039 | 1.015 | 1.077 | 0.987 |
| F | 0.291 | 0.307 | 0.280 | 0.249 | 0.296 | 0.322 |
| OH | 0.796 | 0.977 | 0.946 | 0.653 | 0.888 | 0.489 |
| Σ X-sites | 2.106 | 2.264 | 2.265 | 1.917 | 2.260 | 1.798 |

Mean and point analyses (1–5) of pyromorphite. Coefficients of empirical formulae were calculated assuming (As + P + S + Si) = 3; $H_2O$* contents were calculated based on charge balance.

**Tab. 16** Chemical composition of schultenite from Jáchymov (wt. %)

| | mean | 1 | 2 | 3 | 4 | 5 |
|---|---|---|---|---|---|---|
| FeO | 0.01 | 0.01 | 0.03 | 0.00 | 0.01 | 0.00 |
| PbO | 64.27 | 64.91 | 64.63 | 64.55 | 64.02 | 63.23 |
| ZnO | 0.03 | 0.00 | 0.00 | 0.05 | 0.00 | 0.12 |
| $Al_2O_3$ | 0.10 | 0.00 | 0.10 | 0.06 | 0.27 | 0.08 |
| $SiO_2$ | 0.03 | 0.04 | 0.02 | 0.02 | 0.00 | 0.05 |
| $As_2O_5$ | 32.59 | 33.79 | 32.67 | 30.86 | 32.43 | 33.19 |
| $P_2O_5$ | 0.04 | 0.00 | 0.06 | 0.04 | 0.04 | 0.04 |
| $H_2O$* | 2.56 | 2.66 | 2.57 | 2.43 | 2.55 | 2.62 |
| Total | 99.62 | 101.41 | 100.09 | 98.00 | 99.32 | 99.33 |
| $Fe^{2+}$ | 0.001 | 0.000 | 0.001 | 0.000 | 0.001 | 0.000 |
| $Pb^{2+}$ | 1.012 | 0.987 | 1.014 | 1.074 | 1.014 | 0.976 |
| $Zn^{2+}$ | 0.001 | 0.000 | 0.000 | 0.002 | 0.000 | 0.005 |
| $Al^{3+}$ | 0.007 | 0.000 | 0.007 | 0.005 | 0.019 | 0.005 |
| Σ M-site | 1.021 | 0.987 | 1.023 | 1.081 | 1.034 | 0.987 |
| $Si^{4+}$ | 0.001 | 0.002 | 0.001 | 0.001 | 0.000 | 0.003 |
| $As^{5+}$ | 0.997 | 0.998 | 0.996 | 0.997 | 0.998 | 0.995 |
| $P^{5+}$ | 0.002 | 0.000 | 0.003 | 0.002 | 0.002 | 0.002 |
| Σ T-site | 1.000 | 1.000 | 1.000 | 1.000 | 1.000 | 1.000 |
| $OH^-$ | 0.999 | 1.002 | 1.000 | 1.002 | 1.001 | 1.002 |

Coefficients of empirical formulae were calculated assuming (As + P + Si) = 1 *apfu*;
$H_2O$* contents were calculated on the basis of ideal composition.

### 4.7. Schultenite

Schultenite forms very rare white to creamy acicular or irregular aggregates up to several mm in size, in association with mimetite and segnitite. The mineral was identified on the basis of electron-microprobe data. Besides dominant Pb and As, very minor amounts of Fe, Zn, Al, P and Si were determined (Tab. 16). The chemical composition corresponds to an empirical formula $(Pb_{1.01}Al_{0.01})_{\Sigma 1.02}(AsO_3OH)_{1.00}$ on the basis of P + As + Si = 1 *apfu*.

### 4.8. Metazeunerite

Metazeunerite was found as bright green well-formed tabular crystals (Fig. 12) up to 1 mm in size in cavities of altered quartz gangue in association with mimetite, cerussite and segnitite. It was identified by powder X-ray diffraction; its refined unit-cell parameters agree very well with the published data for this mineral phase (Tab. 17).

The chemical composition of metazeunerite (Tab. 18) is characterised by minor contents of Zn (up to 0.07 *apfu*), P (up to 0.11 *apfu*) and Si (up to 0.03 *apfu*), in addition to dominant Cu and As. The chemical composition corresponds to an empirical formula $(Cu_{1.05}Zn_{0.05})_{\Sigma 1.10}(UO_2)_{2.16}[(AsO_4)_{1.91}(PO_4)_{0.08}(SiO_4)_{0.01}]_{\Sigma 2.00}.8H_2O$ on the basis of P + As + Si = 2 *apfu*.

## 5. Comments on the conditions of origin of the studied mineral association

The mineral association described here represents an assemblage of alteration phases formed *in situ* in the

**Fig. 12** Well-formed tabular crystal of metazeunerite in cavity of strongly supergene altered quartz gangue. Width of area 0.7 mm, photo J. Sejkora.

**Tab. 17** Refined unit-cell parameters for metazeunerite from Jáchymov (for orthorhombic space group *P4*/*n*)

| | this paper | Locock and Burns (2003) |
|---|---|---|
| *a* [Å] | 7.103(7) | 7.1094(1) |
| *c* [Å] | 17.4157(2) | 17.416(1) |
| *V* [Å$^3$] | 878.6(9) | 880.3(1) |

**Tab. 18** Chemical composition of metazeunerite from Jáchymov (wt. %)

| | mean | 1 | 2 | 3 |
|---|---|---|---|---|
| CuO | 7.40 | 8.47 | 6.09 | 7.65 |
| ZnO | 0.33 | 0.31 | 0.51 | 0.17 |
| $SiO_2$ | 0.07 | 0.00 | 0.05 | 0.15 |
| $As_2O_5$ | 19.45 | 19.85 | 18.18 | 20.33 |
| $P_2O_5$ | 0.49 | 0.13 | 0.57 | 0.76 |
| $UO_3$ | 54.82 | 53.49 | 54.44 | 56.52 |
| $H_2O$* | 12.77 | 12.58 | 12.03 | 13.70 |
| Total | 95.23 | 94.83 | 91.86 | 99.28 |
| $Cu^{2+}$ | 1.050 | 1.220 | 0.917 | 1.012 |
| $Zn^{2+}$ | 0.046 | 0.044 | 0.075 | 0.022 |
| Σ Me-site | 1.096 | 1.264 | 0.992 | 1.034 |
| $Si^{4+}$ | 0.012 | 0.000 | 0.009 | 0.026 |
| $As^{5+}$ | 1.910 | 1.979 | 1.895 | 1.861 |
| $P^{5+}$ | 0.077 | 0.021 | 0.095 | 0.113 |
| Σ T-site | 2.000 | 2.000 | 2.000 | 2.000 |
| $U^{6+}$ | 2.163 | 2.143 | 2.281 | 2.079 |
| $H_2O$ | 8.001 | 8.001 | 8.001 | 8.002 |

Coefficients of empirical formula were calculated on the basis (As + P + Si) = 2 *apfu*;
$H_2O$* contents were calculated on the basis of ideal content of 8 $H_2O$ (Locock and Burns 2003).

supergene zone of an ore vein. The primary vein filling probably consisted of a lens of ores, including massive galena, sphalerite, arsenic and/or arsenopyrite. Such a primary mineral association was described from the Jáchymov ore district by Ondruš et al. (2003b), who interpreted the galena occurrences as being related to uraninite and arsenides. The presence of former uranium minerals, most likely uraninite, is indicated by an alteration product metazeunerite and significant presence of $UO_3$ in wulfenite. According to the nature of the samples studied, we suppose that the vein was intensively leached in acidic oxidizing environment. These low pH conditions suggest that some iron sulphide (e.g. pyrite, marcasite, pyrrhotite or arsenopyrite) must have been a minor primary phase, as such sulphides are commonly required to produce acidic supergene conditions (e.g., Evangelou and Zhang 1995; Johnson and Hallberg 2005; Mihaljevič et al. 2010). Almost all primary minerals, besides sparse remnants of massive galena and sphalerite, were leached out and only the most resistant gangue mineral, quartz, is still present. No As-bearing primary mineral has been found and all As in the system studied is concentrated by supergene minerals. The presence of rare schultenite indicates rather acidic conditions characterized by relatively high activity of dissolved Pb and As and low activity of Cl in the solution (Magalhães and Silva 2003). As these authors concluded, schultenite and anglesite occupy the same low-pH stability field, whereas mimetite and cerussite take over under neutral and basic conditions. Mimetite will probably dominate if the activity of Pb and especially As are relatively high, compared to dissolved $CO_2$. The stability field of philipsbornite–segnitite (alunite supergroup) in the $Pb^{2+}$ and $Cu^{2+}$ containing system (with Cu being subordinate in our case) was discussed by Leverett et al. (2003). They showed that philipsbornite is the stable phase under acidic conditions (pH < 4), whereas mimetite should form under weakly acidic to alkaline conditions (pH ~ 4–8) (for activities of $Pb^{2+}_{aq}$ and $Cu^{2+}_{aq}$ equal to $10^{-8}$ and $10^{-3}$ at 298.2 K).

From the visual inspection of the samples we can propose the following crystallization sequence for the studied phases. The oxidation and leaching of the primary sulphide phases (including probably pyrite/marcasite, further galena, arsenic, etc.) initially led to an increased activity of $H^+$, $Pb^{2+}$, $(AsO_3OH)^{2-}$, $(SO_4)^{2-}$, $Al^{3+}$, $Fe^{3+}$, $Cu^{2+}$ and other elements in the solution. The subsequent formation of supergene phases stable under acidic oxidizing conditions took place locally (minerals of philips bornite–segnitite series, anglesite and schultenite), probably where Pb was elevated. The nature and origin of hydrous solutions instrumental in leaching out the hypogene minerals is unclear. It is certain, however, that such waters were acidic and the activity of $Cl^-$ was low. It appears that minerals of the mimetite–pyromorphite series are younger, as they form crusts covering the older philipsbornite–segnitite grains. This stage represented an increase in pH values, possibly due to exhaustion of acidic solutions producing iron sulphides, and elevated $Cl^-$ and $F^-$ activity (halides most probably derived from apatite dissolution in surrounding rocks). Bajda (2010)

proved that mimetite is more soluble than previously considered, based on work of Inegbenebor et al. (1989). Bajda (2010) presented new thermodynamic data and suggested that dissolved $AsO_4^{3-}$ species are most frequent above pH = 8 in the Pb–$As^{+5}$–Cl system (activity of dissolved $Pb_{tot} = 10^{-8}$, $Cl_{tot} = 10^{-3}$, partial pressure of $CO_2 = 10^{-3.5}$ $p_{atm}$); $PbCO_3$ is dominant above pH of 6 (activity of dissolved $As_{tot}^{5+} = 10^{-8}$, $Cl_{tot} = 10^{-3}$, partial pressure of $CO_2 = 10^{-3.5}$ $p_{atm}$). The $MoO_4^{2-}$ anion is the prevalent species in the solution in the system Mo–H–S–O (300 K, 1 bar, concentration of $Mo = 10^{-8}$, $S = 10^{-3}$) under weakly acidic (pH = 4) to strongly alkaline (pH = 14) oxidizing conditions (Ryzhenko 2010). Hence we conclude that the younger association of supergene minerals including mimetite, pyromorphite, cerussite and wulfenite crystallized from weakly acidic to alkaline, oxidized solutions. The source were probably oxidizing waters descending along veins, whereas the primary iron sulphide minerals were leached out, therefore not able to release any further acid ions into solution. The described mineral associations represent fairly stable phases under such conditions.

*Acknowledgements.* The authors thank Boris Ekrt (National Museum, Prague) and Stanislav Vrána (Czech Geological Survey, Prague) for their kind support of this study. This work was financed by the Ministry of Culture of the Czech Republic (MK00002327201 to JS and IJ) and a long-term research plan of Ministry of Education of the Czech Republic (MSM0021620857 to IC and MSM0021622412 [INCHEMBIOL] to RS). Both the referees, Ralph Bottrill and John M. Hughes, as well as handling editor Stuart Mills and editor-in-chief Vojtěch Janoušek, are acknowledged for comments and suggestions that helped greatly to improve the manuscript.

*Electronic supplementary material.* The *cif* file with a table of structure factors (Appendix 1) is available online at the Journal web site (*http://dx.doi.org/10.3190/jgeosci.100*).

## References

Altomare A, Cascarano G, Giacovazzo C, Guagliardi A, Burla CM, Polidori G, Camalli M (1994) SIRPOW.92 – a program for automatic solution of crystal structures by direct methods. J Appl Crystallogr 27: 435–436

Antao SM, Hassan I (2009) The orthorhombic structure of $CaCO_3$, $SrCO_3$, $PbCO_3$ and $BaCO_3$: linear structural trends. Canad Mineral 47: 1245–1255

Bajda T (2010) Solubility of mimetite $Pb_5(AsO_4)_3Cl$ at 5–55 °C. Environ Chem 7: 268–278

Birch WD, Pring A, Gatehouse BM (1992) Segnitite, $PbFe_3H(AsO_4)_2(OH)_6$, a new mineral in the lusungite group from Broken Hill, New South Wales, Australia. Amer Miner 77: 656–659

Bischoff W (1999) Segnitit von St. Andreasberg im Harz. Aufschluss 50: 102–104

Brese NE, O'Keeffe M (1991) Bond-valence parameters for solids. Acta Crystallogr B47: 192–197

Brown ID, Altermatt D (1985) Bond-valence parameters obtained from a systematic analysis of the inorganic crystal structure database. Acta Crystallogr B41: 244–247

Brown ID, Shannon RD (1973) Empirical bond–strength bond–length curves for oxides. Acta Crystallogr A29: 266–282

Chevrier G, Giester G, Heger G, Jarosch D, Wildner M, Zemann J (1992) Neutron single-crystal refinement of cerussite, $PbCO_3$, and comparison with other aragonite-type carbonates. Z Kristallogr 199: 69–74

Dai Y, Hughes JM (1989) Crystal structure refinements of vanadinite and pyromorphite. Canad Mineral 27: 189–192

Dai Y, Hughes JM, Moore PB (1991) The crystal structures of mimetite and clinomimetite, $Pb_5(AsO_4)_3Cl$. Canad Mineral 29: 369–376

David J, Jansa J, Novák F, Prachař I (1990) Philipsbornite from the Sn–W deposit Cínovec in Krušné hory Mts. (Czechoslovakia). Věst Ústř úst geol 65: 367–369

Evangelou VP, Zhang YL (1995) A review: pyrite oxidation mechanisms and acid mine drainage prevention. Environ Sci Technol 25: 141–199

Flis J, Borkiewicz O, Bajda T, Manecki M, Klasa J (2010) Synchrotron-based X-ray diffraction of the lead apatite series $Pb_{10}(PO_4)_6Cl_2$–$Pb_{10}(AsO_4)_6Cl_2$. J Synch Rad 17: 207–214

Giusepetti G, Tadini C (1989) Beudantite: $PbFe_3(SO_4)(AsO_4)(OH)_6$, its crystal structure, tetrahedral site disordering and scattered Pb distribution. Neu Jb Mineral, Mh 27–33

Hashimoto H, Matsumoto T (1998) Structure refinements of two natural pyromorphites, $Pb_5(PO_4)_3Cl$, and crystal chemistry of chlorapatite group, $M_5(PO_4)_3Cl$. Z Kristallogr 213: 585–590

Hoppe R (1979) Effective coordination numbers (ECoN) and mean fictive ionic radii (MEFIR). Z Kristallogr 150: 23–52

Inegbenebor AI, Thomas JH, Williams PA (1989) The chemical stability of mimetite and distribution coefficients for pyromorphite–mimetite solid-solutions. Mineral Mag 53: 363–371

Jacobsen SD, Smyth JR, Swope JR, Downs RT (1998) Rigid-body character of $SO_4$ groups in celestine, anglesite and barite. Canad Mineral 35: 1053–1060

Jansa J, Novák F, Pauliš P, Scharmová M (1998) Supergene minerals of the Sn–W deposit Cínovec, Krušné hory Mountains (Czech Republic). Bull mineral-petrolog Odd Nár Muz (Praha) 6: 83–112 (in Czech)

Johnson DB, Hallberg KB (2005) Acid mine drainage remediation options: a review. Sci Tot Environ 338: 3–14

Kolitsch U, Pring A (2001) Crystal chemistry of the crandallite, beudantite and alunite groups: a review and evaluation of the suitability as storage materials for toxic metals. J Miner Petrol Sciences 96: 67–78

Krivovichev SV, Brown ID (2001) Are the compressive effects of encapsulation an artefact of the bond valence parameters? Z Kristallogr 216: 245–247

Krivovichev SV, Chernyshov DY, Döbelin N, Armbruster T, Kahlenberg V, Kaindl R, Ferraris G, Tessadri R, Kaltenhauser G (2006) Crystal chemistry and polytypism of tyrolite. Amer Miner 91: 1378–1384

Laugier J, Bochu B (2007) LMGP – Suite of Programs for the Interpretation of X-ray Experiments. Accessed on September 19, 2011, at *http://www.ccp14.ac.uk/tutorial/lmgp/*

Leverett P, McKinnon AR, Williams PA (2003) Mineralogy of the oxidized zone at the New Cobar ore body. In: Roach IC (ed) Advances in Regolith. CRC LEME, Bentley, pp 267–270

Locock AJ, Burns PC (2003) Crystal structures and synthesis of the copper-dominant members of the autunite and meta-autunite groups: torbernite, zeunerite, metatorbernite and metazeunerite. Canad Mineral 41: 489–502

Lugli C, Medici L, Saccardo M (1999) Natural wulfenite: structural refinement by single-crystal X-ray diffraction. Neu Jb Mineral, Mh: 281–288

Magalhães MCF, Silva MCM (2003) Stability of lead(II) arsenates. Invited review. Monatsh Chem 134: 735–743

Mihaljevič M, Ettler V, Šebek O, Drahota P, Strnad L, Procházka R, Zeman J, Šráček O (2010) Alteration of arsenopyrite in soils under different vegetation covers. Sci Total Environ 408: 1286–1294

Mills SJ (2007) The Crystal Chemistry and Geochronology of Secondary Minerals from the Broken Hill Deposit, New South Wales. Unpublished Ph.D. thesis, University of Melbourne, Melbourne, pp 1–249

Miyake M, Minato I, Morikawa H, Iwai S-H (1978) Crystal structures and sulphate force constants of barite, cerussite, and anglesite. Amer Miner 63: 506–510

Momma K, Izumi F (2008) VESTA: a three-dimensional visualization system for electronic and structural analysis. J Appl Crystallogr 41: 653–658

Morin G, Juillot F, Ildefonse P, Calas G, Samama JC, Chevallier P, Brown JG (2001) Mineralogy of lead in a soil developed on a Pb-mineralized sandstone Largentière, France. Amer Miner 86: 92–104

Ondruš P, Veselovský F, Hloušek J, Skála R, Vavřín I, Frýda J, Čejka J, Gabašová A (1997) Secondary minerals of the Jáchymov (Joachimsthal) ore district. J Czech Geol Soc 42: 3–6

Ondruš P, Veselovský F, Gabašová A, Hloušek J, Šrein V (2003a) Geology and hydrothermal vein system of the Jáchymov (Joachimsthal) ore district. J Czech Geol Soc 48: 3–18

Ondruš P, Veselovský F, Gabašová A, Hloušek J, Šrein V, Vavřín I, Skála R, Sejkora J, Drábek M (2003b) Primary minerals of the Jáchymov ore district. J Czech Geol Soc 48: 19–147

Ondruš P, Veselovský F, Gabašová A, Hloušek J, Šrein V (2003c) Supplement to secondary and rock-forming minerals of the Jáchymov ore district. J Czech Geol Soc 48: 149–155

Ondruš P, Veselovský F, Gabašová A, Drábek M, Dobeš P, Malý K, Hloušek J, Sejkora J (2003d) Ore-forming processes and mineral parageneses of the Jáchymov ore district. J Czech Geol Soc 48: 157–192

Ondruš P, Skála R, Veselovský F, Sejkora J, Vitti C (2003e) Čejkaite, the triclinic polymorph of $Na_4(UO_2)(CO_3)_3$ – a new mineral from Jáchymov, Czech Republic. Amer Miner 88: 686–693

Petříček V, Dušek M, Palatinus L (2006) Jana2006. The Crystallographic Computing System. Institute of Physics, Prague, Czech Republic. Accessed on July 1, 2011 at *http://jana.fzu.cz/*

Plášil J, Sejkora J, Čejka J, Škácha P, Goliáš V (2009a) Supergene mineralization of the Medvědín uranium deposit, Krkonoše Mountains, Czech Republic. J Geosci 54: 15–56

Plášil J, Čejka J, Sejkora J, Hloušek J, Goliáš V (2009b) New data for metakirchheimerite from Jáchymov (St. Joachimsthal), Czech Republic. J Geosci 54: 373–384

Plášil J, Čejka J, Sejkora J, Škácha P (2009c) The question of water content in parsonsite: a model case – occurrence at the Červené žíly vein system, Jáchymov (St. Joachimsthal), Czech Republic. J. Geosci 54: 385–394

Plášil J, Čejka J, Sejkora J, Škácha P, Goliáš V, Jarka P, Laufek F, Jehlička J, Němec I, Strnad L (2010a) Widenmannite, a rare uranyl lead carbonate: occurrence, formation and characterization. Mineral Mag 74: 97–110

Plášil J, Sejkora J, Čejka J, Novák M, Viñals J, Ondruš P, Veselovský F, Škácha P, Jehlička J, Goliáš V, Hloušek J (2010b) Metarauchite, $Ni(UO_2)_2(AsO_4)_2 \cdot 8H_2O$, from Jáchymov, Czech Republic, and Schneeberg, Germany: a new member of the autunite group. Canad Mineral 48: 335–350

Plášil J, Dušek M, Novák M, Čejka J, Císařová I, Škoda R (2011) Sejkoraite-(Y), a new member of the zippeite group containing trivalent cations from Jáchymov (St. Joachimsthal), Czech Republic: description and crystal structure refinement. Amer Miner 96: 983–991

Pouchou JL, Pichoir F (1985) " PAP" (φρZ) procedure for improved quantitative microanalysis. In: Armstrong JT (ed) Microbeam Analysis. San Francisco Press, pp 104–106

Rattray KJ, Taylor MR, Bevan DJM, Pring A (1996) Compositional segregation and solid solution in the

lead-dominant alunite-type minerals from Broken Hill, N.S.W. Mineral Mag 60: 779–785

Robinson K, Gibbs GV, Ribbe PH (1971) Quadratic elongation: a quantitative measure of distortion in coordination polyhedra. Science 172: 567–570

Ryzhenko BN (2010) Technology of groundwater quality prediction: 1. Eh–pH diagram and detention coefficient of molybdenum and tungsten in aqueous solutions. Geochem Int 48: 433–441

Schmetzer K, Tremmel G, Medenbach O (1982) Philipsbornite $PbAl_3H[(OH)_6(AsO_4)_2]$ from Tsumeb, Namibia – a second occurrence. Neu Jb Mineral, Mh: 248–254

Secco L, Nestola F, Dal Negro A (2008) The wulfenite–stolzite series: centric or acentric structures? Mineral Mag 72: 987–900

Sejkora J, Čejka J, Šrein V, Novotná M, Ederová J (1998) Minerals of the plumbogummite–philipsbornite series from Moldava deposit, Krušné hory Mts., Czech Republic. Neu Jb Mineral, Mh 4:145–163

Sejkora J, Čejka J, Šrein V (2001a) Pb dominant members of crandallite group from Cínovec and Moldava deposits, Krušné hory Mts. (Czech Republic). J Czech Geol Soc 46: 53–67

Sejkora J, Houzar S, Šrein V (2001b) Segnitite from Štěpánov nad Svratkou, western Moravia. Acta Mus Moraviae, Sci geol 86: 85–92 (in Czech)

Sejkora J, Škovíra J, Čejka J, Plášil J (2009) Cu-rich members of the beudantite–segnitite series from the Krupka ore district, the Krušné hory Mountains, Czech Republic. J Geosci 54: 355–371

Sejkora J, Ondruš P, Novák M (2010a) Veselovskýite, triclinic $(Zn,Cu,Co)Cu_4(AsO_4)_2(AsO_3OH)_2.9H_2O$, a Zn-dominant analogue of lindackerite. Neu Jb Mineral, Abh 187: 83–90

Sejkora J, Plášil J., Císařová I, Hloušek J (2010b) Unusual fibrous mimetite from the Rovnost mine, Jáchymov (St. Joachimsthal), Czech Republic. Acta Mineral Petrograph, Abstract Series 6: 351

Sejkora J, Plášil J, Ondruš P, Veselovský F, Císařová I, Hloušek J (2010c) Slavkovite, $Cu_{13}(AsO_4)_6(AsO_3OH)_4.23H_2O$, a new mineral species from Horní Slavkov and Jáchymov, Czech Republic: description and crystal structure determination. Canad Mineral 48: 1157–1170

Sheldrick GM (2008) A short history of SHELX. Acta Crystallogr A64: 112–122

Szymański JT (1988) The crystal structure of beudantite, $Pb(Fe,Al)_3[(As,S)O_4]_2(OH)_6$. Canad Mineral 26: 923–932

Škácha P, Goliáš V, Sejkora J, Plášil J, Strnad L, Škoda R, Ježek J (2009) Hydrothermal uranium-base metal mineralization of the Jánská vein, Březové Hory, Příbram, Czech Republic: lead isotopes and chemical dating of uraninite. J Geosci 54: 1–13

Tvrdý J, Plášil J (2010) Jáchymov – reiche Erzlagerstätte und Radonbad im böhmischen Westerzgebirge. Aufschluss 61: 277–292

Walenta K (1966) Beiträge zur Kenntnis seltener Arsenatmineralien unter besonderer Berücksichtigung von Vorkommen des Schwarzwaldes. Tschermaks Mineral Petr Mitt 11: 121–161

Walenta K, Zwiener M, Dunn PJ (1982) Philipsbornit, ein neues Mineral der Crandallitreihe von Dundas auf Tasmanien. Neu Jb Mineral, Mh 1–5

Williams PA (1990) Oxide Zone Geochemistry. Ellis Horwood, Chichester, pp 1–286